**SANDIA REPORT**
SAND2009-1217
Unlimited Release
Printed April 2009

# A Simplified Model of $TiH_{1.65}/KClO_4$ Pyrotechnic Ignition

Ken S. Chen

Prepared by
Sandia National Laboratories
Albuquerque, New Mexico 87185 and Livermore, California 94550

Sandia is a multiprogram laboratory operated by Sandia Corporation,
a Lockheed Martin Company, for the United States Department of Energy's
National Nuclear Security Administration under Contract DE-AC04-94AL85000.



Issued by Sandia National Laboratories, operated for the United States Department of Energy by Sandia Corporation.



Available to DOE and DOE contractors from
U.S. Department of Energy
Office of Scientific and Technical Information
P.O. Box 62
Oak Ridge, TN 37831

Telephone: (865) 576-8401
Facsimile: (865) 576-5728
E-Mail: reports@adonis.osti.gov
Online ordering: http://www.osti.gov/bridge

Available to the public from
U.S. Department of Commerce
National Technical Information Service
5285 Port Royal Rd.
Springfield, VA 22161

Telephone: (800) 553-6847
Facsimile: (703) 605-6900
E-Mail: orders@ntis.fedworld.gov
Online order: http://www.ntis.gov/help/ordermethods.asp?loc=7-4-0#online

SAND2009-1217
Unlimited Release
Printed April 2009

# A Simplified Model of $TiH_{1.65}/KClO_4$ Pyrotechnic Ignition

Ken S. Chen
Nanoscale and Reactive Processes Department
Sandia National Laboratories
P.O. Box 5800
Albuquerque, New Mexico 87185-0836

**Abstract**

A simplified model was developed and is presented in this report for simulating thermal transport coupled with chemical reactions that lead to the pyrotechnic ignition of $TiH_{1.65}/KClO_4$ powder. The model takes into account Joule heating via a bridgewire, thermal contact resistance at the wire/powder interface, convective heat loss to the surroundings, and heat released from the $TiH_{1.65}$− and $KClO_4$−decomposition and $TiO_2$−oxidation reactions. Chemical kinetic sub-models were put forth to describe the chemical reaction rate(s) and quantify the resultant heat release. The simplified model predicts pyrotechnic ignition when heat from the pyrotechnic reactions is accounted for. Effects of six key parameters on ignition were examined. It was found that the two reaction-rate parameters and the thermal contact resistance significantly affect the dynamic ignition process whereas the convective heat transfer coefficient essentially has no effect on the ignition time. Effects of the initial/ambient temperature and electrical current load through the wire are as expected. Ignition time increases as the initial/ambient temperature is lowered or the wire current load is reduced. Lastly, critical needs such as experiments to determine reaction-rate and other model-input parameters and to measure temperature profiles, time to ignition and burn-rate data for model validation as well as efforts in incorporating reaction-rate dependency on pressure are pointed out.

## Acknowledgments

The author would like to thank Everett Hafenrichter (2522), Marcia Cooper (2554), Tom Massis (2555), Anita Renlund (2550), Dean Dobranich (1514), Mael Baer (1500), and Ken Erickson (1512) for helpful technical discussions on $TiH_{1.65}/KClO_4$ pyrotechnic ignition and related topics. The author also wants to thank Mike Hobbs and Bill Erikson (both 1516) for helps with chemistry implementation in Calore. Moreover, the author acknowledges Mike Hobbs' expert assistance in adiabatic flame temperature estimation. Lastly, the author is thankful to Dean Dobranich and Mike Hobbs for performing peer review of this report and their helpful comments.

# CONTENTS

# 1. INTRODUCTION*

Actuators employing the mechanism of bridgewire-activated pyrotechnic ignition are widely used in nuclear weapons. Consequently, it is critically important to elucidate the key physical and chemical phenomena that lead to pyrotechnic ignition or cause ignition failure. Figure 1 schematically shows the simplified axisymmetric geometry of the bridgewire-activated pyrotechnic ignition problem. The essential physical and chemical phenomena are as follows:

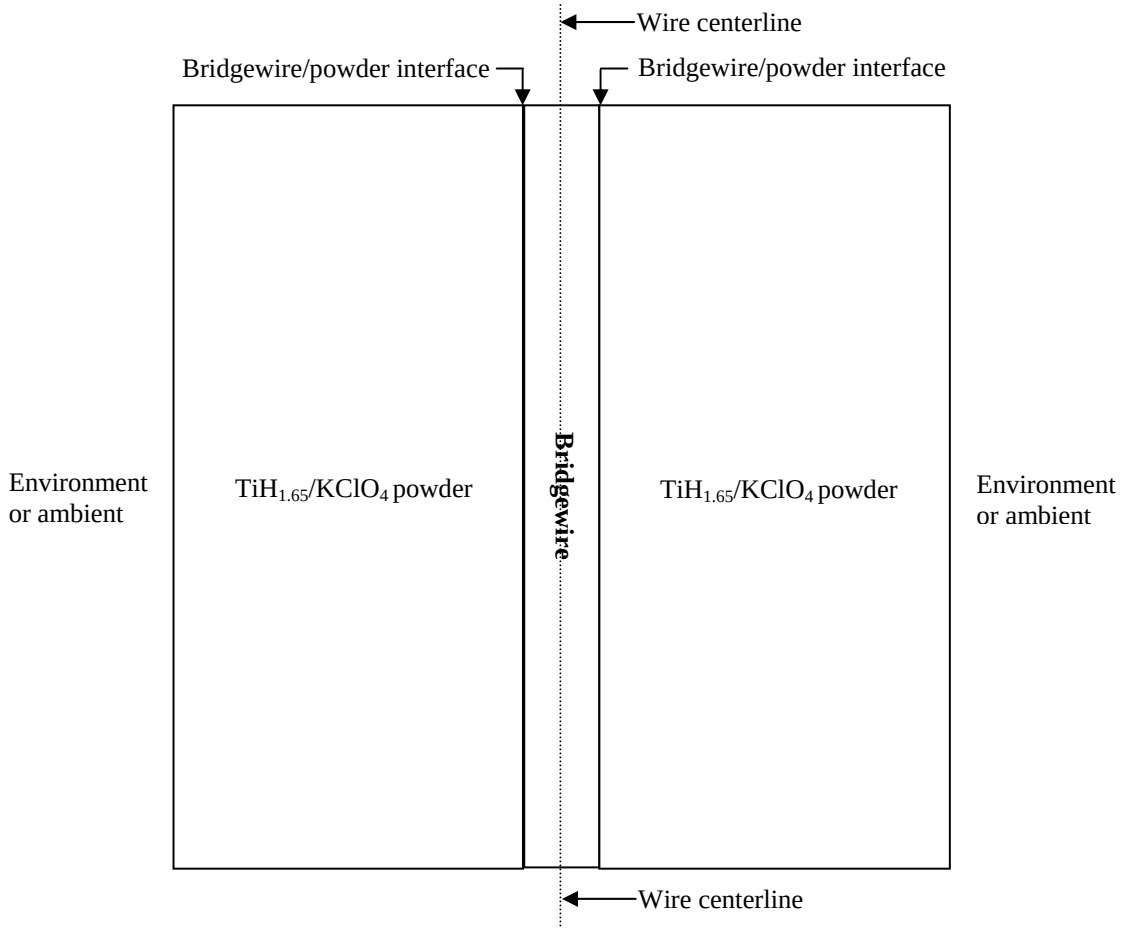


Figure 1. Simplified axisymmetric geometry of bridgewire-activated pyrotechnic ignition (not to scale)

1) electric current is applied through the bridgewire and a volumetric heat source via Joule heating is generated within; 2) heat is conducted from the bridgewire to the $TiH_{1.65}/KClO_4$ powder after overcoming the thermal contact resistance at the wire/powder interface; 3) as heat is conducted within the powder, decomposition of $TiH_{1.65}$ and $KClO_4$ powder, oxidation of Ti and $TiO_2$, and formation of $H_2O$ take place while heat is released mainly from the $TiO_2$-oxidation

* This report is based on a technical memorandum by the author issued on January 5, 2009.

reaction but also from the $H_2O$-formation reaction; and 4) heat is lost to the surrounding environment from the outer surface. The present work was built upon the previous work of Dean Dobranich[1] and took into account the essential phenomena as described above, particularly the chemical reactions.

## 2. REACTION MECHANISMS

### 2.1 Four-step reaction mechanism

The bridgewire-activated pyrotechnic ignition process can be described by the following four reaction steps[2,3,4,5] (on a mole basis):

i) Decomposition of potassium perchlorate ($KClO_4$) oxidizer at temperature > 583 K (310 °C):

$$KCLO_4\,(s) \rightarrow KCl\,(s) + 2O_2\,(g) \qquad (1).$$

ii) Decomposition of titanium subhydride ($TiH_{1.65}$) at temperature > 698 K (425 °C):

$$TiH_{1.65}\,(s) \rightarrow Ti\,(s) + 0.825\,H_2(g) \qquad (2).$$

iii) Formation of water ($H_2O$) vapor at $TiH_{1.65}$ decomposition temperature > 698 K:

$$2H_2\,(g) + O_2\,(g) \rightarrow 2\,H_2O\,(g) \qquad (3).$$

iv) Oxidation of titanium (Ti) to titanium dioxide ($TiO_2$) at temperature > 793 K

$$Ti\,(s) + O_2\,(g) \rightarrow TiO_2\,(s) \qquad (4).$$

For convenience of notation, we shall let

| | | | |
|---|---|---|---|
| $A = KCLO_4\,(s)$, | $B = TiH_{1.65}\,(s)$, | $C = KCl\,(s)$, | $D = H_2O\,(g)$, |
| $E = TiO_2\,(s)$, | $F = O_2\,(g)$, | $G = H_2\,(g)$, | $H = Ti\,(s)$. |

Using the above short-hand notations, Reactions 1 – 4 can be rewritten as:

$$A \rightarrow C + 2\,F \qquad (5),$$

$$B \rightarrow H + 0.825\,G \qquad (6),$$

$$2\,G + F \rightarrow 2\,D \qquad (7),$$

$$H + F \rightarrow E \qquad (8).$$

For convenience of implementation in the Calore thermal response code, we convert Reactions (5) – (8) to a mass-fraction basis:

$$A \rightarrow 0.538\ C + 0.462\ F \quad (9),$$

$$B \rightarrow 0.9664\ H + 0.0336\ G \quad (10),$$

$$G + 7.936\ F \rightarrow 8.936\ D \quad (11),$$

$$H + 0.6685\ F \rightarrow 1.6685\ E \quad (12).$$

From Equations 9 – 12, we can obtain the following Stoichiometric Matrix, which is needed in the Calore implementation:

| Reaction: | 1 | 2 | 3 | 4 |
|---|---|---|---|---|
| Species | | | | |
| A | −1.0 | 0 | 0 | 0 |
| B | 0 | −1.0 | 0 | 0 |
| C | 0.538 | 0 | 0 | 0 |
| D | 0 | 0 | 8.936 | 0 |
| E | 0 | 0 | 0 | 1.6685 |
| F | 0.462 | 0 | −7.936 | −0.6685 |
| G | 0 | 0.0336 | −1.0 | 0 |
| H | 0 | 0.9664 | 0 | −1.0 |
| | ——— | ——— | ——— | ——— |
| Sum: | 0 | 0 | 0 | 0 |

For reactions expressed on a mass-fraction basis, column entries in the Stoichiometric Matrix should sum to zero. This is the case for all four columns as shown above. Here, each column represents one reaction.

For simplicity, we shall take all reactions to be first order, so we have:

$$r_1 = k_1 A \quad (13)$$

$$r_2 = k_2 B \quad (14)$$

$$r_3 = k_3 GF \quad (15)$$

$$r_4 = k_4 HF \quad (16).$$

From these assumed reaction rate expressions, we obtain the following Reaction Matrix, which is also required in the Calore implementation:

| | $r_1$ | $r_2$ | $r_3$ | $r_4$ |
|---|---|---|---|---|
| A | 1 | 0 | 0 | 0 |
| B | 0 | 1 | 0 | 0 |
| C | 0 | 0 | 0 | 0 |
| D | 0 | 0 | 0 | 0 |
| E | 0 | 0 | 0 | 0 |
| F | 0 | 0 | 1 | 1 |
| G | 0 | 0 | 1 | 0 |
| H | 0 | 0 | 0 | 1 |

From the JANAF Thermochemical Tables[6], we obtain the following values of *heat of formation*:

| | Heat of Formation (kcal/mole) |
|---|---|
| KCl at 600 K (327 °C): | –104.561 |
| $KClO_4$ at 600 K (327 °C): | –97.595 |
| $TiH_{1.65}$ at 700 K (427 °C): | –27.9 |
| $H_2O$ at 700 K (427 °C): | –68.3 |
| $TiO_2$ between 700 K (427 °C) and 900 K (627 °C): | ~ –225 |

Tom Massis[3] has also reported similar values of heat of formation for these chemical compounds. Using the above *heat of formation* data, we obtain the following values of *heat of reaction*:

| | Heat of reaction (kcal/mole) | Heat of reaction (J/mole) |
|---|---|---|
| Reaction 1 at 600 K (327 °C): | –4.92 | –20,585 |
| Reaction 2 at 700 K (427 °C): | 27.9 | 116,734 |
| Reaction 3 at 700 K (427 °C): | –56.3475 | –235,758 |
| Reaction 4 at 700 K − 900 K: | –225 | –941,400 |

## 2.2 One-step reaction mechanism

A one-step overall reaction can be readily obtained by adding Reactions (1) – (4), on a mole basis:

$$0.70625\ KCLO_4\,(s) + TiH_{1.65}\,(s) \rightarrow 0.70625\ KCl\ (s) + 0.825\ H_2O\ (g) + TiO_2\,(s) \qquad (17).$$

Or on a mass-fraction basis:

$$KCLO_4\,(s) + 0.5062\ TiH_{1.65}\,(s) \rightarrow 0.5381\ KCl\ (s) + 0.1519\ H_2O\ (g) + 0.8162\ TiO_2\,(s) \qquad (18).$$

For convenience, we introduce the following short-hand notation, on a mass-fraction basis:

$$\overline{A} = 0.664\ KCLO_4\,(s) + 0.336\ TiH_{1.65}\,(s)$$
$$\overline{B} = H_2O\ (g)$$
$$\overline{C} = 0.397\ KCl\ (s) + 0.603\ TiO_2\,(s)$$

Now, the overall reaction can be rewritten on a mass-fraction basis as:

$$\overline{A} \rightarrow 0.1\,\overline{B} + 0.9\,\overline{C} \qquad (19).$$

This indicates that 1 gram of (66.4wt%−$KCLO_4$/33.6wt%−$TiH_{1.65}$) powder produces 0.1 gram of gaseous $H_2O$ and 0.9 gram of (39.7wt%−KCl/60.3wt%−$TiO_2$) solid mixture.

The Stoichiometric Matrix (on mass basis) for the one-step overall reaction is as follows:

| Reaction | 1 |
|---|---|
| Species | |
| $\overline{A}$ | -1.0 |
| $\overline{B}$ | 0.1 |
| $\overline{C}$ | 0.9 |

Similarly, for simplicity, we shall take the overall reaction to be first order, so we have:

$$r_1 = k_1 \overline{A} \qquad (20).$$

From the above reaction rate expression, we can obtain the following Reaction Matrix:

| | $\underline{r_1}$ |
|---|---|
| $\overline{A}$ | 1 |
| $\overline{B}$ | 0 |
| $\overline{C}$ | 0 |

From Equation 19, we obtain the following heat of reaction for the one-step overall reaction:

$H_{rxn,overall}$ = – 7.004 kJ (per gram of 33.6wt%−$TiH_{1.65}$/66.4wt%−$KCLO_4$ mixture)

= – 1.674 kcal (per gram of 33.6wt%−$TiH_{1.65}$/66.4wt%−$KCLO_4$ mixture).

The above heat of reaction *means* that 1.674 kcal of heat is released per gram of 33.6wt%−$TiH_{1.65}$/66.4wt%−$KCLO_4$ powder. This value is in close agreement with the average measured value of 1.609 kcal (per gram of 33wt%−$TiH_{1.65}$/67wt%−$KCLO_4$ powder) as reported by Tom Massis[3]. As described below, Burchett[7] reported an average density of 2.38 g/cm$^3$ for the $TiH_{1.65}$/$KClO_4$ powder with loading pressure ranging from 4 kpsi to 20 kpsi. Using this average powder density value, the volumetric heat of reaction for the one-step overall reaction is $1.667 \cdot 10^{10}$ J/(m$^3$ of $TiH_{1.65}$/$KClO_4$ powder).

## 3. REACTION RATE CONSTANT DEPENDENCE ON TEMPERATURE

It is customary to describe the temperature dependence of reaction rate constants ($k_1, k_2, k_3$, and $k_4$ in Equations 13 – 16 and $k_1$ in Equation 20) by employing the Arrhenius equation:

$$k = Ae^{-\frac{E}{RT}} \qquad (21)$$

where $A$ is the pre-exponential factor, $E$ is the activation energy, $T$ is temperature, and $R$ is the universal gas constant ($\equiv 8.314$ J/mole-K). Clearly, the Arrhenius equation requires two parameters, $A$ and $E$.

## 4. GOVERNING EQUATIONS AND BOUNDARY CONDITIONS

In the present work, the thermal transport in both the bridgewire and the $TiH_{1.65}/KClO_4$ powder regions is taken to be by conduction with volumetric Joule heating in the wire and volumetric heating in the powder due to the homogeneous exothermic chemical reaction(s). Accordingly, the transient temperature profile within the wire and powder regions is governed by[8]

$$\frac{\partial(\rho c T)}{\partial t} = \nabla \cdot (\kappa \nabla T) + \dot{q} \tag{22}$$

where $T$ is temperature, $t$ time, $\rho$ density, $c$ specific heat, $\kappa$ thermal conductivity, and $\dot{q}$ the volumetric heat source. For the wire region, $\dot{q} = P / V_{wire}$ where $P$ is the Joule heating power given in Equation 23 below and $V_{wire}$ wire volume. For the powder region, $\dot{q} = \sum_{i=1}^{n} r_i q_{rxn,i}$ where $r_i$ is the reaction rate for the $i^{th}$ reaction, $q_{rxn,i}$ the heat of reaction for the $i^{th}$ reaction, and $n$ the number of reactions. For the one-step reaction mechanism, $n$ = 1.

In the present work, we follow Dean Dobranich[1] and use the following expression for estimating the heating power provided by the bridgewire:

$$P = I^2 R_0 [1 + \alpha_0 (T - T_0)] \tag{23}$$

where $P$ is the Joule heating power, $I$ is applied electric current, $T$ is wire temperature, $T_0$ is the reference temperature, $\alpha_0$ is the effective wire resistivity, and $R_0$ is the effective wire resistance. The values of $T_0$, $\alpha_0$, and $R_0$ as given by Dean Dobranich[1] are 300 K, 0.00011721 $K^{-1}$, and 0.79502067 Ω, respectively. With the Joule heating power supplied by Equation 23, Calore computes the volumetric heat source in the wire region. Similarly, with the volumetric heat of reaction(s) provided, Calore computes the volumetric heat source in the powder region, which is due to the homogeneous pyrotechnic chemical reaction(s). There is some small amount of Joule heating in the powder adjacent to the wire, but this is neglected.

In the present work, we focus on the thermal transport in the radial direction (i.e., normal to the wire surface) and ignore any variation along the length of the wire. As such, we only need to specify the boundary conditions at the wire/powder interface and at the outer surface

from which heat is lost to the environment. At the wire/powder interface, a thermal contact resistance is prescribed to account for the imperfect contact between the bridgewire and the $TiH_{1.65}/KClO_4$ powder. At the outer surface, a heat transfer coefficient is specified to describe the heat loss to the surrounding environment as follows:

$$-k\frac{\partial T}{\partial r} = h(T - T_\infty) \qquad \text{at the outer surface} \qquad (24).$$

## 5. PHYSICAL AND THERMAL PROPERTIES

In the present work, we follow Dobranich[1] and Taylor[9] and take the bridgewire's physical and thermal properties as follows:

Density – 8250 kg/m$^3$,

Specific heat – 448 J/kg-K,

Thermal conductivity – 8 W/m-K.

For the $TiH_{1.65}/KClO_4$ powder, Olden Burchett[7] measured its density as a function of loading pressure and put forth the following correlation relating powder density ($\rho$) to loading pressure ($P$):

$$\rho = \frac{\rho_r}{1 + (\frac{\rho_r}{\rho_0} - 1)\left[1 - \left(\frac{P}{P_0}\right)^{1/b}\right]^{1/a}} \qquad (25)$$

where $a$ = 0.5, $b$ = 2.522, $P_0$ = 409.6 MPa, $\rho_0$ = 1.643 g/cm$^3$, and $\rho_r$ = 2.839 g/cm$^3$. For a loading pressure of 4 kpsi (or $P$ = 27.58 MPa), Equation 25 gives $\rho$ = 2.16 g/cm$^3$ whereas for P = 20 kpsi = 137.9 MPa, ρ = 2.606 g/cm$^3$. Thus, the average density for the $TiH_{1.65}/KClO_4$ powder with loading pressure ranging from 4 kpsi to 20 kpsi is 2.383 g/cm$^3$. Taylor[7] reported a thermal conductivity value of 0.00823 W/(cm-K) or 0.823 W/(m-K). A set of specific heat vs. temperature data were presented by Klassen and Massis[10] along with the following correlation for the $TiH_x/KClO_4$ powder with x ranging from 0 to 2:

$$c = 0.000248T + 0.163 \qquad \text{for} \qquad -50°C \le T \le 150°C \qquad (26)$$

where the specific heat $c$ is in cal/(g-°C) and $T$ is in °C.

## 6. RESULTS AND DISCUSSION

In the present work, by employing Calore we solved Equation 22, which governs the transient process of thermal transport coupled with volumetric Joule heating in the wire and simultaneous heat generation in the powder due to homogeneous exothermic pyrotechnic chemical reaction(s) as well as energy lost to the surrounding environment. Due to the lack of experimental data for determining the reaction rate constants, we decided to employ the simpler one-step overall reaction mechanism (versus the 4-step reaction mechanism) coupled with the simplified geometry in the present work. Consequently, the present simplified Calore-based pyrotechnic-ignition model requires six process parameters: current load, thermal contact resistance, preexponential factor and activation energy, convective heat transfer coefficient, and initial/ambient temperature (in the present work, the initial temperature is taken to be the same as the ambient temperature). In addition, the model needs the following physical and thermal properties for both the bridgewire and the $TiH_{1.65}/KClO_4$ powder: density, specific heat, and thermal conductivity. Physical and thermal properties of the wire and powder used in the present work are listed in Table 1 whereas kinetic and process parameters for the Base Case are listed in Table 2. In the present work, the bridgewire diameter was taken to be 48 microns[1,11] whereas the outer surface of the $TiH_{1.65}/KClO_4$ powder was set at 500 microns (radius) from the wire/powder interface. Lastly, a mesh size of 0.5 micron was employed in both the wire and powder regions. The mesh in the wire region was refined toward the wire/powder interface whereas a uniform mesh size was used in the powder region in order to follow the ignition front. To ensure that the ignition be captured, an initial time step of $10^{-10}$ second and an automatic adaptive time integration scheme were employed. A typical run took approximately 160 seconds of CPU time on a HP xw8400 Workstation to simulate the ignition process for duration of 10 milliseconds.

### 6.1 Base Case

Computed temperature profiles for the Base Case are shown in Figures 1, 2, and 3. Wire temperature along the radial direction at various times is displayed in Figure 1 whereas

powder temperature along the radial direction at various times is presented in Figure 2. Powder temperatures at various locations as functions of time are shown in Figure 3. Figures 2 and 3 clearly show that ignition occurs at the wire/powder interface at 2.922 milliseconds (ms) with parameters employed in the Base Case; at this time, Figure 1 shows that wire temperature rises toward the wire/powder interface due to heat generated from the powder ignition at the interface. Before ignition occurs, wire temperature decreases along the radial direction from the wire centerline to the interface due to heat loss at the outer surface to the surrounding environment.

Let's examine Figure 3 in more detail. Figures 3a and 3b show the computed powder temperature as a function of time at different locations with the former displaying temperature at locations close to the wire/powder interface (10, 20, 30, 40, and 50 μm, respectively, from the wire/powder interface) and the latter at locations farther away (100, 200, 300, 400, and 500 μm, respectively, from the wire/powder interface). Clearly, the ignition front starts at the wire/powder interface and moves toward the outer surface. In the present work, chemistry is activated (i.e., chemical reactions are initiated) when the temperature reaches 320 K (which has been set somewhat arbitrarily in the present study. Experiment is needed to determine this initiation temperature above which ignition reactions start to occur). Strictly speaking, this initiation temperature should be a local one. But due to a structural coding "bug" in Calore, which was uncovered recently by Andy Kraynik[13] and requires substantial effort to fix[†], chemistry is activated when the maximum temperature (which is located in the wire center before ignition occurs), instead of when the local temperature reaches 320 K. Consequently, chemistry was activated earlier than it should and this effect becomes more visible as the distance from the wire/powder interface increases. Fortunately, the temperature drop within the wire is very small as can be seen from Figure 1 such that the effect of the Calore coding bug on the computed ignition time at the wire/powder interface is negligibly small. Since for the Base Case the ignition time at the wire/powder interface is 2.922 ms and that at the outer surface (500 μm from the wire/powder interface) is 4.992 ms (see Figure 3b), the burn rate in the Base Case is thus approximately 242 μm/ms or 24.2 cm/s. This burn rate is about 10 times of that for potassium perchlorate ($KCLO_4$) alone[2]. One would expect that adding titanium subhydride ($TiH_{1.65}$) to

[†] Request for fixing this coding bug has been submitted and the Calore Team is currently looking into this problem.

potassium perchlorate should raise the burn rate. In any case, to validate the burn rate for the $TiH_{1.65}/KClO_4$ powder, experimental data is certainly needed.

Figure 3b shows a plateau temperature of 4725 K. This temperature plateau is due to the ignition at the wire/powder interface and subsequent conductive burn at the adiabatic flame temperature. Using the ideal gas law as the equation of state and considering all possible product species generated with KCl and $H_2O$ being the leading gaseous products, the adiabatic flame temperature is estimated to be around 3250 K[16,17,18]. The difference between the plateau temperature in Figures 3b and the adiabatic flame temperature estimated with the assumptions of ideal gas and KCl and $H_2O$ being the leading gaseous products can be attributed to $TiO_2$ also present as the major product in the $TiH_{1.65}/KClO_4$ pyrotechnic ignition process that was modeled in this work.

## 6.2 Effects of reaction-rate parameters

As is indicated by Equation 21, the reaction rate constant for the overall reaction (Equation 17 or 18) depends on two parameters: pre-exponential factor (A) and activation energy (E). Figures 4 and 5 show the effects of the pre-exponential factor on, respectively, powder temperature and the time to ignition at the wire/powder interface. Clearly, the pre-exponential factor significantly impacts the ignition time. As the pre-exponential factor increases, the ignition time decreases dramatically when $\log(A) < 12$. Moreover, the shape of the powder temperature profile also changes as A is reduced. As the pre-exponential factor becomes sufficiently small, one can expect from Figure 4 that ignition will not occur. In Figures 4 and 5, log(A) is varied over a wide range: from 8 to 20 such that the base-case value ($\log(A) = 15$) is somewhat in the middle of this range. The low limit of $\log(A) = 8$ was so chosen as to show that ignition will not occur within 15 ms.

Figures 6 and 7 show the effects of the activation energy on, respectively, powder temperature and the time to ignition at the wire/powder interface. It is interesting to note that the shape of the powder temperature profile remains about the same as E varies. The ignition time, however, does lengthen as E is raised. The activation energy value of 100,000 J/mole used in the Base Case is a reasonable one as compared with similar propellant powder materials. For example, the activation energy as measured by DTA (differential thermal analysis) for the thermal decomposition of ammonium perchlorate ($NH_4ClO_4$) is reported to

be 134,000 J/mole. In Figures 6 and 7, the activation energy is varied from 60,000 to 180,000 J/mole, which is a wide range.

## 6.3 Effects of thermal contact conductance

Figures 8 and 9 show the effects of the thermal contact conductance on, respectively, powder temperature and the time to ignition at the wire/powder interface. It is seen from the two figures that the thermal contact conductance has significant effect on ignition time, particularly when the thermal contact conductance is less than 500,000 W/($m^2$-K). One can also infer from Figure 8 that ignition will not occur when the thermal contact conductance becomes sufficiently small (or the thermal contact resistance becomes sufficiently large).

## 6.4 Effects of convective heat transfer coefficient

Figures 10 and 11 show the effects of the convective heat transfer coefficient on powder temperature, respectively, at the wire/powder interface and the outer surface. Clearly, varying the convective heat transfer coefficient has no effect on the ignition times (at the wire/powder interface or at the outer surface). Moreover, varying the convective heat transfer coefficient has little effect on the profile of the powder temperature at the wire/powder interface. Raising the convective heat transfer coefficient, however, does lower the powder temperature after ignition and this is expected. Lastly, the heat transfer coefficient seems to have no effect on the burn rate.

## 6.5 Effects of initial/ambient temperature

Figures 12 and 13 show the effects of initial/ambient temperature on powder temperature at the wire/powder interface and the time to ignition at various locations within the powder region. As mentioned previously, the initial and ambient temperatures are taken to be the same in the present work. Plainly from Figures 12 and 13, lowering the initial/ambient temperature simply lengthens the time to ignition at the wire/powder interface and shifts the powder-temperature profile to the right.

## 6.6 Effects of wire current load

Figures 14 and 15 show the effects of the electrical current load through the wire. Clearly, the time to ignition at the wire/powder interface increases with decreasing current load, as expected. The sharp rise in temperature (which is indicative of ignition) is still observed even when the current load is reduced to 1.8 A (which is 54.5% of that in the Base Case) though the ignition

time is relatively long at approximately 23ms. In other words, ignition can still occur when the current load is less than 1.8 A but the ignition time may become unacceptably long.

## 7. SUMMARY/CONCLUSIONS AND REMARKS ON FUTURE WORK

A simplified model was developed for simulating thermal transport coupled with chemical reactions that lead to the pyrotechnic ignition of $TiH_{1.65}/KClO_4$ powder. The model takes into account Joule heating via a bridgewire, thermal contact resistance at the wire/powder interface, convective heat loss to the surroundings, and heat released from the $TiH_{1.65}$− and $KClO_4$−decomposition and $TiO_2$−oxidation reactions. Chemical kinetic sub-models were put forth to describe the chemical reaction rate(s) and quantify the resultant heat release. Using a reduced kinetic model that describes the one-step overall pyrotechnic reaction, the simplified model was demonstrated in a basecase simulation and parametric studies were carried out to examine effects of six key parameters (pre-exponential factor, activation energy, thermal contact resistance, convective heat transfer coefficient, initial/ambient temperature, and wire current load) on ignition. It was found that the two reaction-rate parameters and the thermal contact resistance significantly affect the dynamic ignition process whereas the convective heat transfer coefficient essentially has no effect on the ignition time. Effects of the initial/ambient temperature and electrical current load through the wire are as expected: ignition time increases as the initial/ambient temperature is lowered or the current load is reduced.

There are several areas that require future efforts. First, experiments are needed to determine the reaction-rate constants (pre-exponential factor and activation energy). The reaction-rate constants employed in the basecase study were so chosen as to yield the ignition time at the wire/powder interface of about 3 ms. The pre-exponential factor of $10^{15}$ $s^{-1}$ and the activation energy of $10^5$ J/mole seem to be reasonable values but these parameters have been found based on calibration simulations and may not be valid for other conditions. Experiments are also needed to measure the burn rate of the $TiH_{1.65}/KClO_4$ powder in order to provide data for model validation. Secondly, the dependence of the reaction rate on pressure (due to the generation of the gaseous product in the $TiH_{1.65}$− and $KClO_4$−decomposition and water-formation reactions) needs to be taken into account in order to be able to simulate the "ignition quenching" phenomena. Such a pressure-dependent kinetic model has been

demonstrated in Calore by Mike Hobbs (1516) for simulating foam decomposition[14] and the implementation of this type of model in Aria for explosive-decomposition application is being pursued currently by Bill Erikson (1516)[15]. Once the pressure dependence is taken into account using the reduced kinetic model (which describes the one-step overall reaction), it may be helpful to implement the 4-step reaction mechanism so that its effect on the ignition dynamics can be examined. Lastly, the structural coding "bug" in Calore, which results in the chemistry being activated earlier than it should (particularly in locations away from the wire/powder interface), needs to be fixed so as to yield more reasonable and accurate ignition times and burn rate.

## 8. REFERENCES


1. D. Dobranich, "Speculations on actuator failures at low temperatures", *Sandia technical memorandum* issued on January 7, 2008.
2. Pyrotechnic Chemistry, K. & B. Kosanke et al., Pyrotechnic Reference Series No. 4, *Journal of Pyrotechnics*, Inc., Whitewater, CO 81527, USA (2004).
3. T. M. Massis, "The processing, properties and use of the pyrotechnic mixture-titanium subhydride/potassium perchlorate", paper presented at the *AIAA, ASME, SAE, and ASEE, Joint Propulsion Conference and Exhibit*, 32nd, Lake Buena Vista, FL, July 1–3, 1996.
4. R. Behrens, Jr., "Reactions leading to the ignition of TiHx/$KCLO_4$ pyrotechnics", unpublished manuscript.
5. M. R. Baer, private discussions.
6. JANAF Thermochemical Tables by Stull & Prophet, 2nd Ed., Project Directors: D. R. Stull and H. Prophet, NSRDS–NBS 37, issued June 1971.
7. O. L. Burchett, R. W. Dietzel, A. P. Montoya "The Compaction Behavior of Ten Pyrotechnic Materials", *Sandia Report*, SAND79-1833 (1979).
8. S. W. Bova, K. D. Copps, and C. K. Newman, "Calore – A Computational Heat Transfer Program", *Theory Manual*, SAND2006-6083 (2006). Also see http://calore.sandia.gov .
9. J. G. Taylor, "Thermal Property Determination for Brigewire Ignition Modeling", *Sandia Report*, SAND83-0877 (1983).
10. S. E. Klassen and T. M. Massis, "Heat capacity measurements on $TiH_x/KClO_4$, x = 0−2", *Sandia technical memorandum* issued on March 22, 1982.
11. K. G. Pierce and J. R. Leith, "A numerical model of the thermal processes leading to ignition in a pyrotechnic device", in Proceedings of the Eleventh International Pyrotechnics Seminar, p. 47−57, IIT Research Institute, Chicago, Illinois (1986).

12. J. P. Holman, Heat Transfer, 5th Edition, p. 13, McGraw-Hill Book Company, NY (1981).

13. A. M. Kraynik, private communication.

14. M. L. Hobbs, "A simple pressurization model for Calore", *Sandia technical memorandum* issued on January 22, 2007.

15. W. W. Erikson, email communication, December 9, 2008.

16. M. L. Hobbs and M. R. Baer, "Nonideal thermoequilibrium calculations using a large product species data base", *Shock Waves*, **2**, 177 – 187 (1992).

17. M. L. Hobbs, M. R. Baer, M. R. Baer, and B. C. McGee, "JCZS: an intermolecular potential database for performing accurate detonation and expansion calculations", *Propellants, Explosives, Pyrotechnics*, **24**, 269 – 279 (1999).

18. M. L. Hobbs, private discussions.

Table 1. Physical and Thermal Properties of Bridgewire & Powder

(Note: the superscripts here denote the reference numbers)

| | Bridgewire | Powder |
|---|---|---|
| Density ($kg/m^3$) | 8250[1] | 2380[7] |
| Specific Heat (J/kg-K) | 448[1] | Equation 25[10] |
| Conductivity (W/m-K) | 8[1] | 0.823[9] |

Table 2. Kinetic and Process Parameters for the Base Case

| | |
|---|---|
| Pre-exponential factor (A), $s^{-1}$ | $10^{15}$ |
| Activation energy, J/mole | $10^5$ |
| Current load (I), A | 3.3 |
| Thermal contact resistance, $m^2$-K/W | $7.5188 \cdot 10^{-6}$ |
| Thermal contact conductance, $W/m^2$-K | $1.33 \cdot 10^5$ |
| Convective heat transfer coefficient ($W/m^2$-K) | 5 |
| Initial/ambient temperature, °C | 0 |

Note: thermal contact conductance, direct input to Calore, is the reciprocal of thermal contact resistance. The value used here is from Dean Dobranich[1]. Taylor[9] has also used a value of $1.333 \cdot 10^5$ $W/m^2$-K.

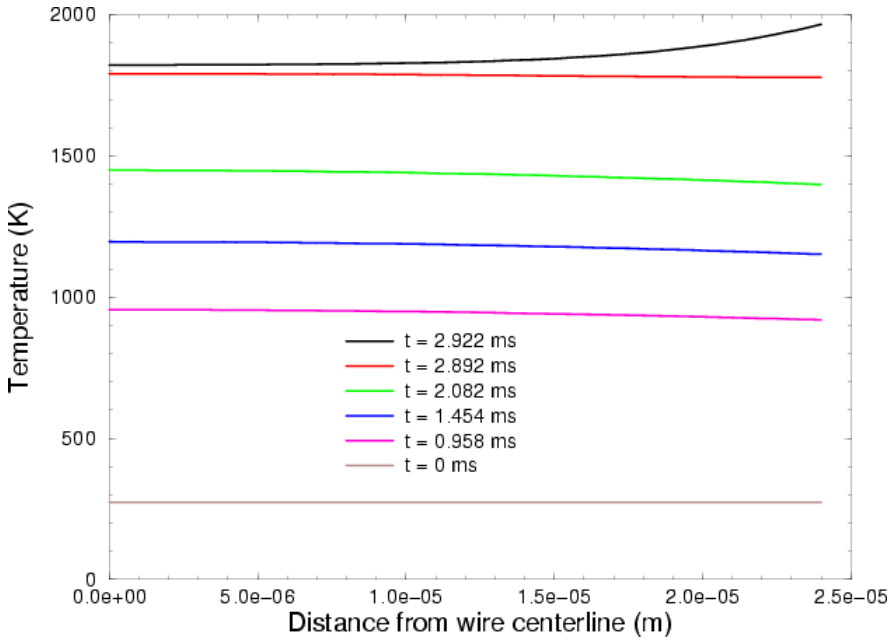


Figure 1. Computed wire temperature along radial distance from wire centerline at various times − from 0 to 2.922 ms (when ignition occurs at the wire/powder interface), Base Case.

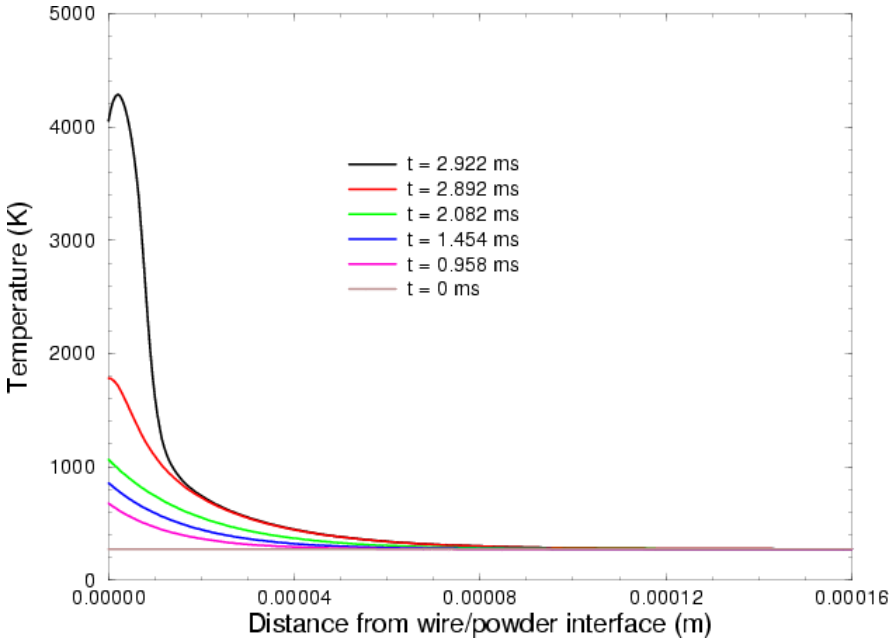


Figure 2. Computed powder temperature along radial distance from wire/powder interface at various times − from 0 to 2.922 ms (when ignition at wire/powder interface occurs), Base Case.

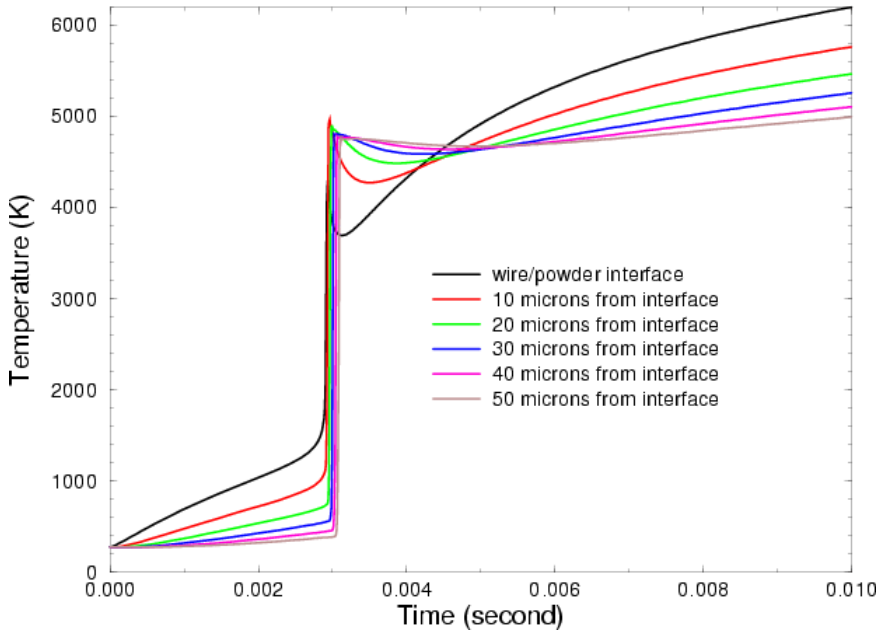


(a)

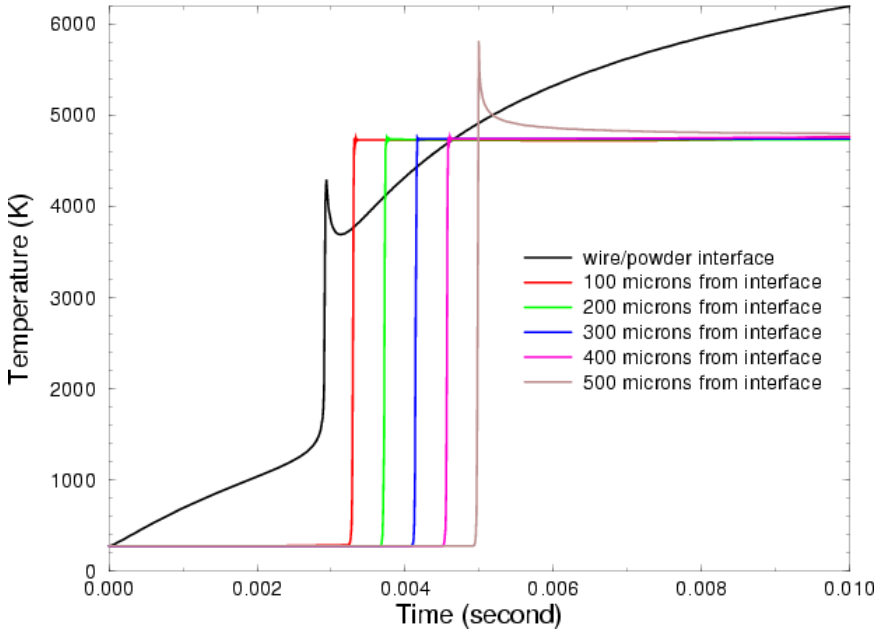


(b)

Figure 3. Temperature in powder region at various locations as functions of time − Base Case
(a) from the interface to 10, 20, 30, 40, 50, and 100 μm away from the interface;
(b) from the interface to 100, 200, 300, 400, and 500 μm away from the interface.

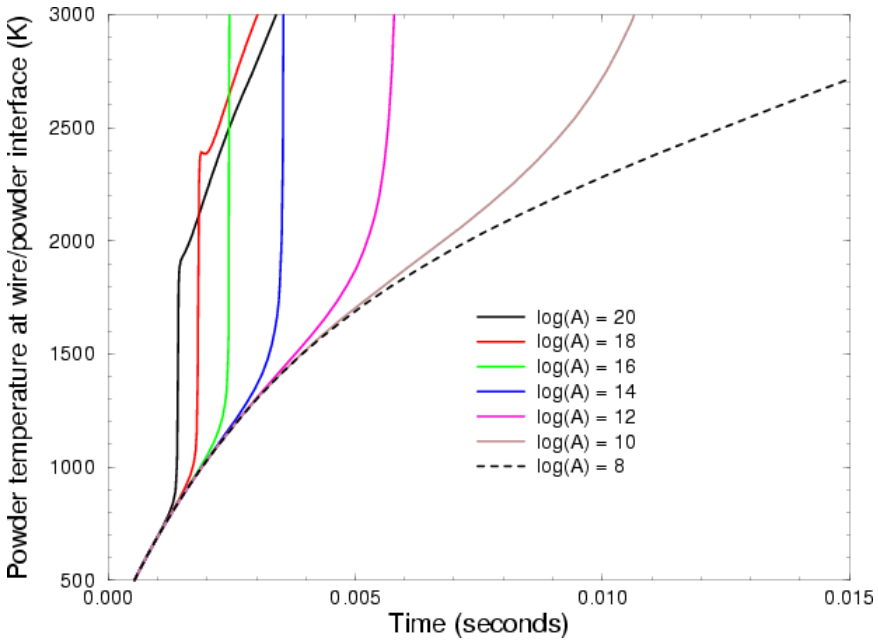


Figure 4. Effect of pre-exponential factor on powder temperature at wire/powder interface

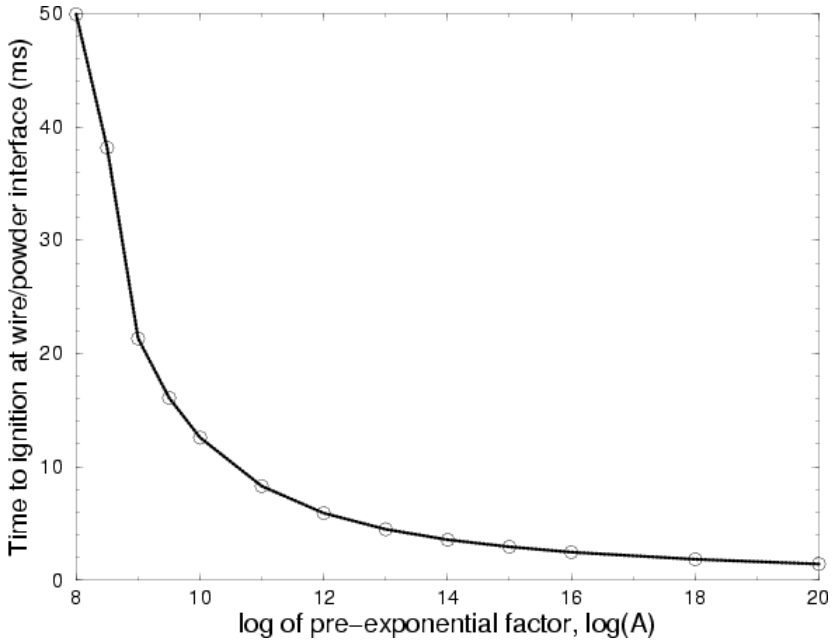


Figure 5. Effect of pre-exponential factor on time to ignition at wire/powder interface

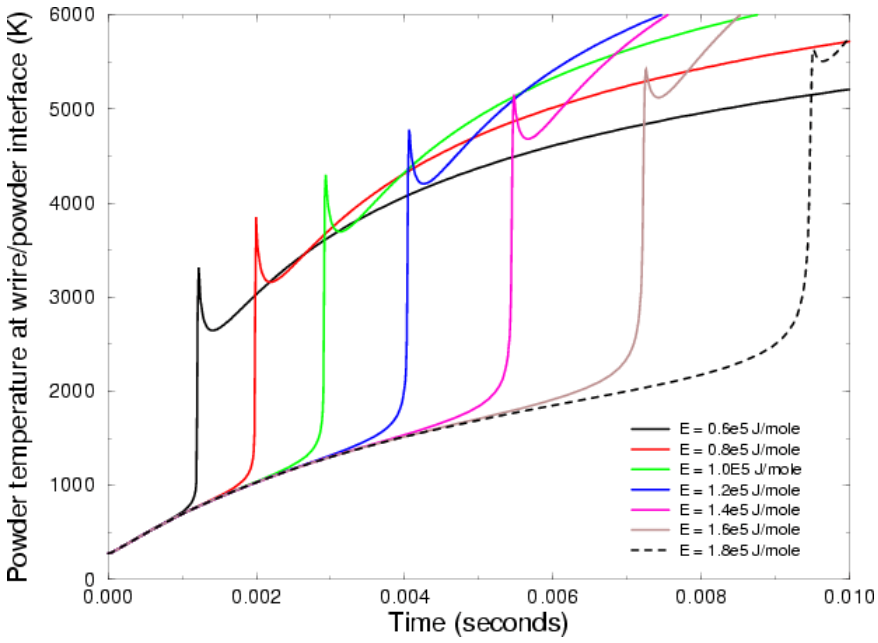


Figure 6. Effect of activation energy on powder temperature at wire/power interface

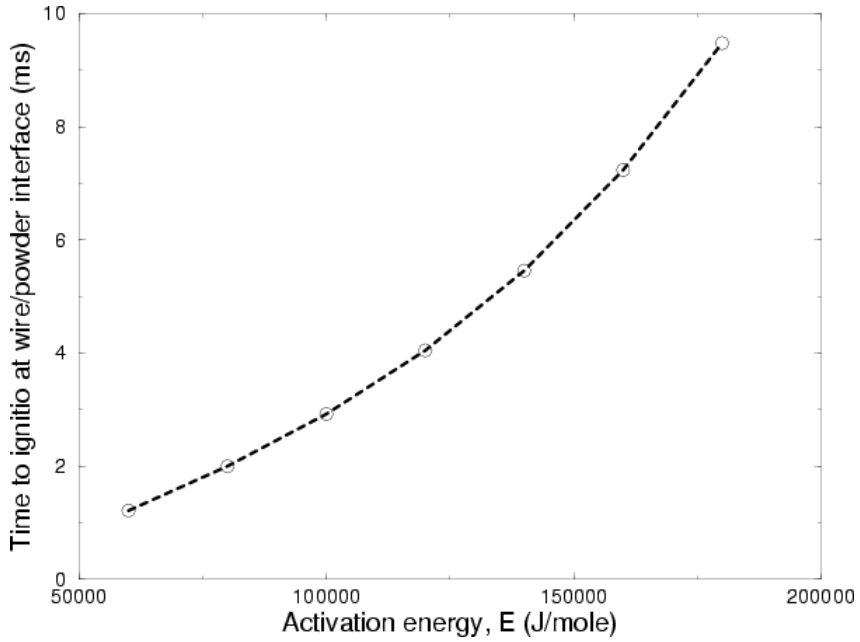


Figure 7. Effect of activation energy on time to ignition at wire/power interface

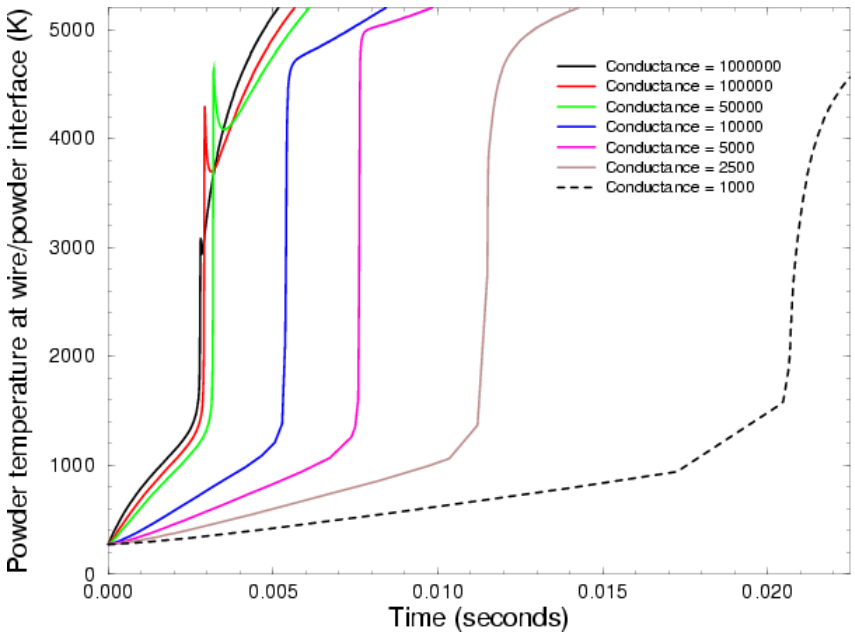


Figure 8. Effect of thermal contact conductance on powder temperature at wire/power interface (note: units of the thermal contact conductance here are in W/m$^2$-K)

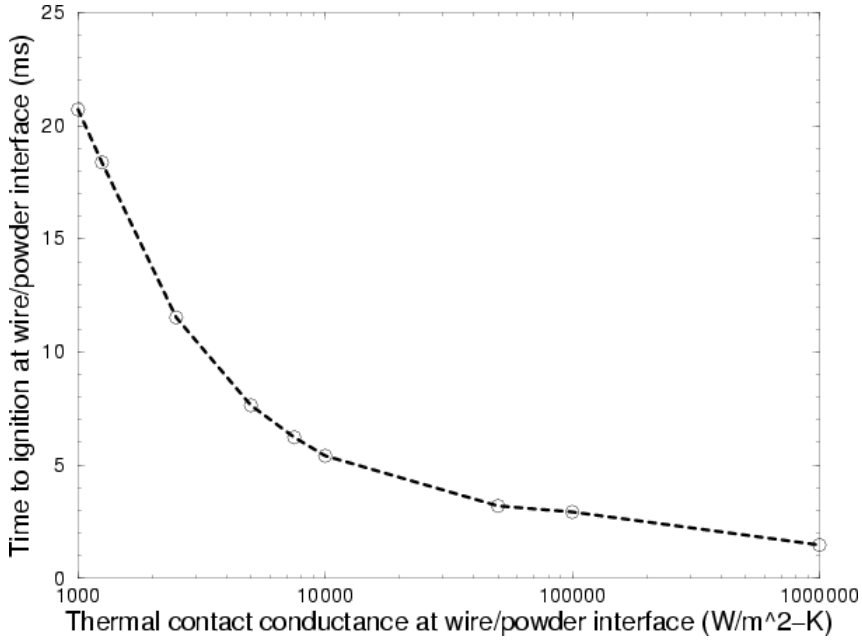


Figure 9. Effect of thermal contact conductance on time to ignition at wire/power interface

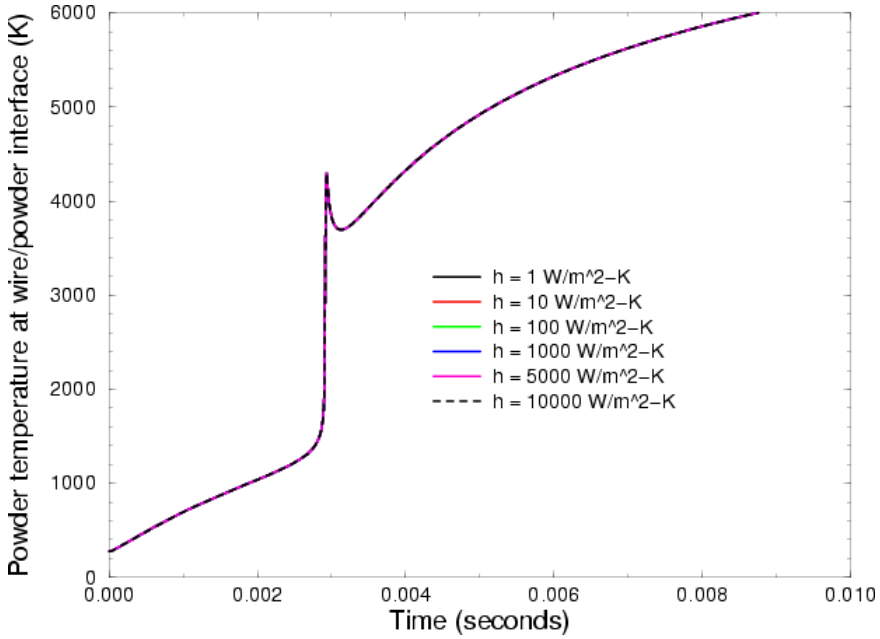


Figure 10. Effect of convective heat transfer coefficient on powder temperature at wire/power interface

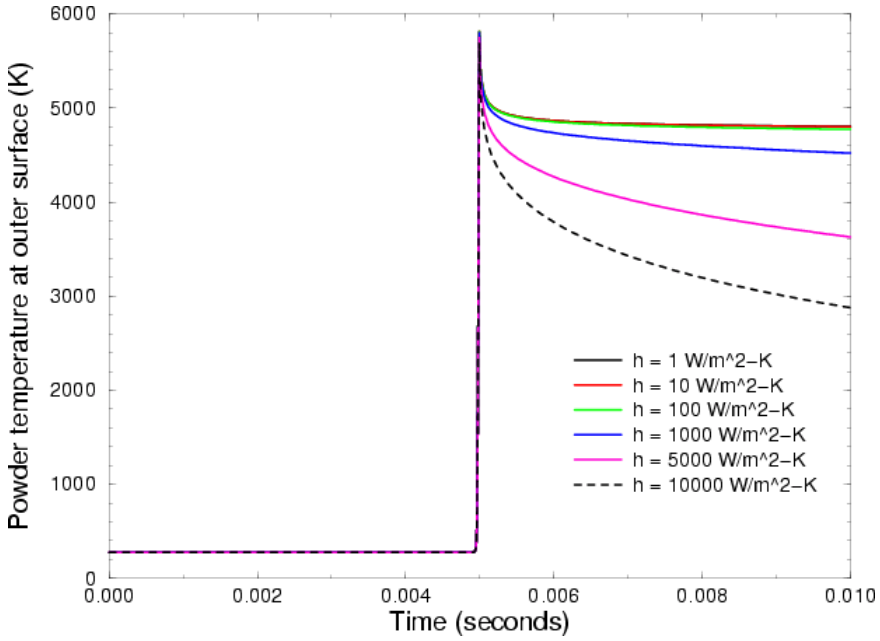


Figure 11. Effect of convective heat transfer coefficient on powder temperature at outer surface

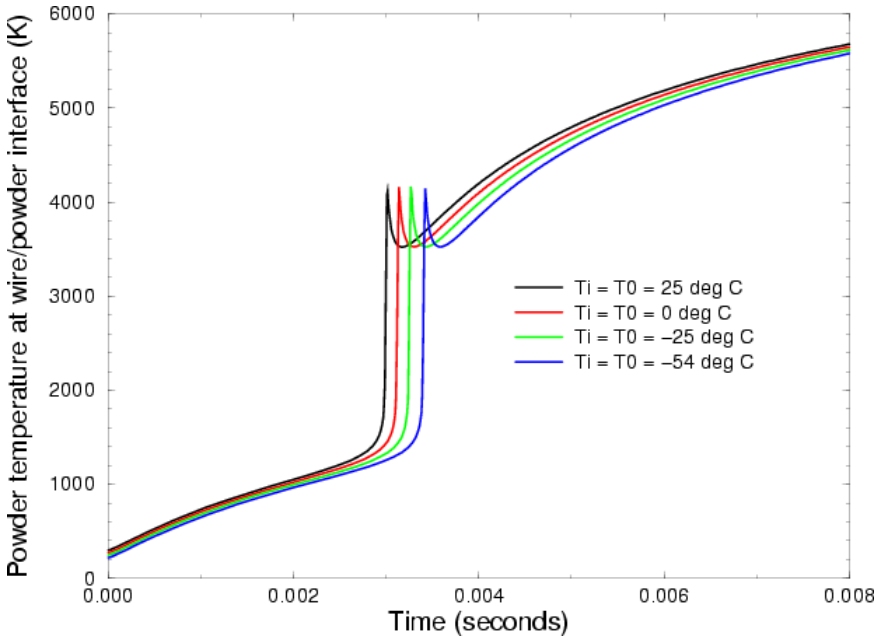


Figure 12. Effect of initial/ambient temperature on powder temperature at wire/powder interface

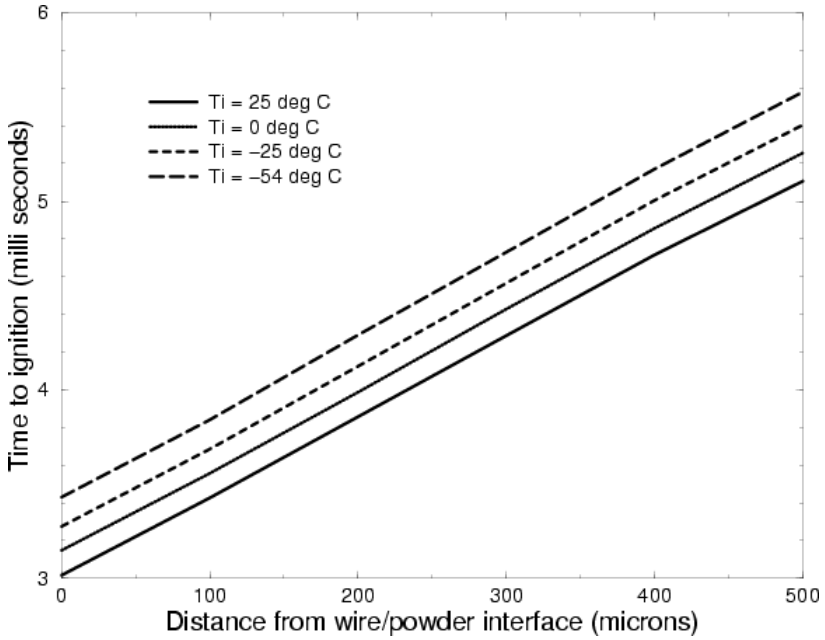


Figure 13. Effect of convective heat transfer coefficient on powder temperature at outer surface

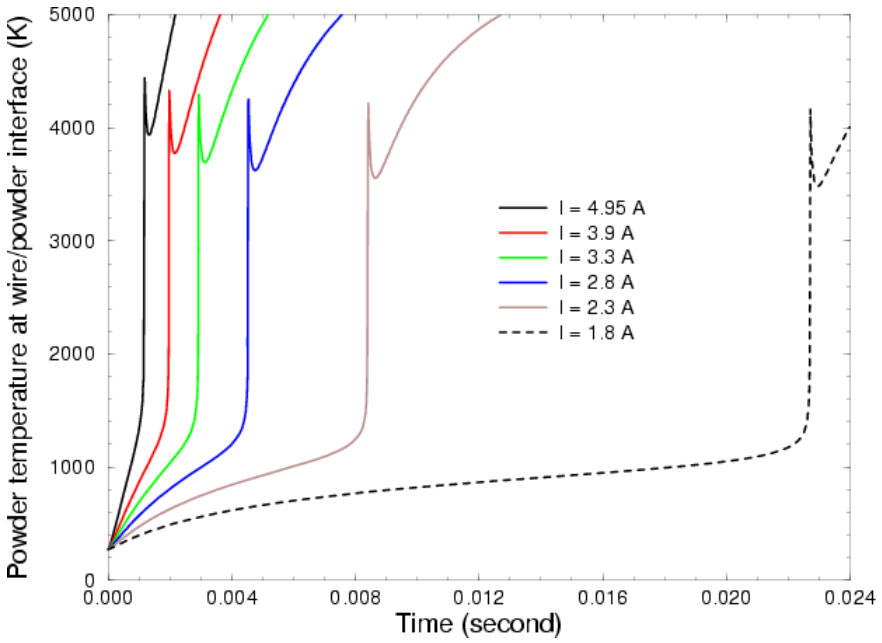


Figure 14. Effect of wire current load on powder temperature at wire/powder interface

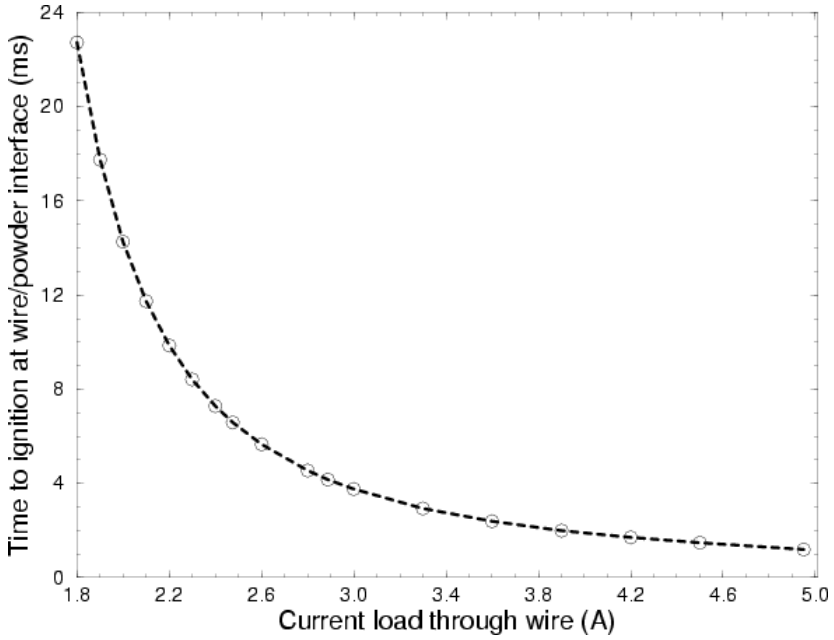


Figure 15. Effect of wire current load on time to ignition at wire/powder interface

## DISTRIBUTION

| | | | |
|---|---|---|---|
| 1 | MS-0836 | J. S. Lash | 1510 |
| 1 | MS-0836 | M. R. Baer | 1500 |
| 1 | MS-0826 | K. L. Erickson | 1512 |
| 1 | MS-0836 | T. L. Aselage | 1514 |
| 1 | MS-0346 | D. Dobranich | 1514 |
| 1 | MS-0836 | M. J. Martinez | 1514 |
| 3 | MS-0836 | K. S. Chen | 1516 |
| 1 | MS-0836 | W. W. Erikson | 1516 |
| 1 | MS-0836 | M. L. Hobbs | 1516 |
| 1 | MS-1454 | A. M. Renlund | 2550 |
| 1 | MS-1452 | E. S. Hafenrichter | 2552 |
| 1 | MS-1454 | M. J. Kaneshige | 2552 |
| 1 | MS-1455 | L. M. G. Minier | 2554 |
| 1 | MS-1454 | M. A. Cooper | 2554 |
| 1 | MS-1455 | T. M. Massis | 2555 |
| 1 | MS-0899 | Technical Library | 9536 (electronic file) |


Sandia National Laboratories